ACS APPLIED MATERIALS & INTERFACES

Research Article

www.acsami.org

Laser-Induced Nondestructive Patterning of a Thin Ferroelectric Polymer Film with Controlled Crystals using $Ge_8Sb_2Te_{11}$ Alloy Layer for Nonvolatile Memory

Insung Bae,[†] Richard Hahnkee Kim,[†] Sun Kak Hwang,[†] Seok Ju Kang,*[,‡] and Cheolmin Park*[,†]

[†]Department of Materials Science and Engineering, Yonsei University, Seoul 120749, Republic of Korea

[‡]Department of Materials Science and Engineering, Hanbat National University, Daejeon 305-719, Korea

Supporting Information

ABSTRACT: We present a simple but robust nondestructive process for fabricating micropatterns of thin ferroelectric polymer films with controlled crystals. Our method is based on utilization of localized heat arising from thin $Ge_8Sb_2Te_{11}$ (GST) alloy layer upon exposure of 650 nm laser. The heat was generated on GST layer within a few hundred of nanosecond exposure and subsequently transferred to a thin poly(vinylidene fluoride-*co*-trifluoroethylene) film deposited on GST layer. By controlling exposure time and power of the scanned laser, ferroelectric patterns of one or two microns in size are fabricated with various shape. In the micropatterned regions, ferroelectric polymer crystals were efficiently controlled in both degree of the crystallinity and the molecular orientations. Nonvolatile memory devices with laser scanned ferroelectric polymer layers exhibited excellent device performance of large remnant polarization, ON/OFF current ratio and data retention. The results are comparable with devices containing ferroelectric films thermally annealed at least for 2 h, making our process extremely efficient for saving time. Furthermore, our approach can be conveniently combined with a number of other functional organic materials for the future electronic applications.

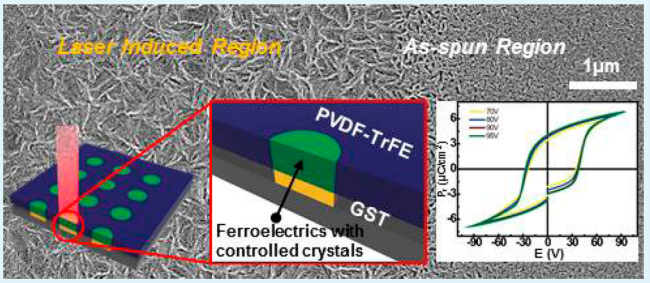

KEYWORDS: *nondestructive patterning, ferroelectric polymer, PVDF-TrFE, nonvolatile polymer memory, $Ge_8Sb_2Te_{11}$ alloy layer, laser-induced writing*

1. INTRODUCTION

An attractive feature of ferroelectric polymers such as poly(vinylidene fluoride) (PVDF) and its copolymers with trifluoroethylene (TrFE) has been considered as a next-generation nonvolatile memory candidate because of its lower production cost, easier fabrication process, and more flexible nature than inorganic ferroelectric materials. The unique molecular polarization between hydrogen and fluorine atoms in PVDF-TrFE, for instance, endows the bistable states, which can switch from one to the other by using electrical bias in the thin film. As a result, various innovative types of PVDF-TrFE based memory devices have been successfully proposed and demonstrated in 2000s to provide their merits for the future memory application.[1−7] Among the many possible systems, Naber et al.[8] reported PVDF-TrFE transistor combined with solution based organic semiconductor which exhibits excellent nonvolatile performance without significant degradation of retention and endurance. In particular, this result led to intensive study on PVDF-TrFE for improving the ferroelectric performance as well as in particular employing the material for ferroelectric field effect transistor (FeFET) architecture.[9−11]

The previous works clearly suggest that the control of PVDF-TrFE crystals in the thin film is of key importance to spur progress of the memory properties. It has been understood that there is a desired molecular orientation of PVDF-TrFE for memory application, that is, carbon−carbon backbone chain should be perpendicular to the electrical bias field otherwise it erodes the cell performance due to the lack of bistability. Hence, various methods have been exerted in controlling the molecular orientation using thermal annealing,[12,13] nano confinement,[10] surface energy control of the substrate[14] and this enables to utilize the PVDF-TrFE materials as a promising ferroelectric memory component. Although the decent memory performance has been demonstrated by many research groups including ours,[2,8−11] from the industrial point of view, a ferroelectric thin film should be properly patterned not only for integrating cells as many as possible but also for minimizing undesired cell-to-cell cross-talk problem.

A variety of micropatterns of PVDF-TrFE have been extensively developed in particular based on printing technologies not to harm ferroelectric properties of the soft polymer including micro/nanoimprinting lithography,[15−22] transfer printing, capillary molding,[23] microcontact printing,[11] phase separation,[24] and using anodic porous alumina

Received: May 30, 2014
Accepted: August 15, 2014
Published: August 15, 2014

membranes.[25−27] These techniques are promising for multiplying tiny cells with the same size and shape but limited to arbitrary patterns. Only a few methods enabled direct writing of micro PVDF-TrFE patterns with arbitrary geometries. Scanned X-ray beam on a thin PVDF-TrFE film successfully changed the molecular conformation of PVDF-TrFE from ferroelectric beta phase to paraelectric alpha one, giving rise to well-defined patterns of alpha crystalline PVDF-TrFE.[28,29] A heated probe of surface probe microscope touched on a thin PVDF-TrFE film allowed the localized melting and recrystallization of PVDF-TrFE, leading to arbitrary patterns with controlled ferroelectric crystals.[30−32] Considering that most of the previous works are so-called destructive with direct interaction of ferroelectric polymer with patterning sources, i.e., X-ray and heated surface probe, it would be beneficial to develop a facile method for fabricating arbitrary micropatterns of ferroelectric polymers in nondestructive manner where the ferroelectric polymers are not directly exposed to patterning sources but intact and thus one can potentially reduce deterioration of the materials.

In this contribution, we developed a new nondestructive patterning method of a thin PVDF-TrFE film by using a $Ge_8Sb_2Te_{11}$ (GST) alloy layer placed beneath the PVDF-TrFE. Our method is based on utilization of localized heat arising from GST layer upon exposure of focused 650 nm laser. The heat resulting from the facile photon-to-phonon conversion of GST provided sufficient mobility of the PVDF-TrFE molecules, giving rise to the increase of degree of crystallinity. In the laser scanned regions, we also observed preferred crystal orientation of edge-on crystalline microdomains whose length and width are approximately 300 and 50 nm closely packed with needle-like shape. Furthermore, the controlled PVDF-TrFE crystals by the laser resulted in the improved ferroelectric properties of the film characterized in both metal/ferroelectric/metal capacitors and FeFETs. Using this strategy, we can create the microsize lines, dots and even arbitrary letters in a few hundred nanoseconds with optimized speed and power of laser.

2. EXPERIMENTAL SECTION

Materials and Film Preparation. A 30 nm thick $Ge_8Sb_2Te_{11}$ (GST) film was deposited by a sputtering system on highly doped silicon gate electrode and supplied by Nanostorage Inc., KOREA. A PVDF-TrFE copolymer with 27.5 wt % TrFE used in this research was kindly supplied by MSI Sensor, PA. PVDF-TrFE films were made by spin coating method (5 wt % solution in methyl ethyl ketone). The ellipsometry was performed under ambient conditions using a spectroscopic ellipsometer (alfa SE, J.A. Woollam) at an angle of incidence of ca. 70°. Film thicknesses were calculated by adapting the experimental data to a bilayer model.

Laser Patterning. A lab-made experimental setup was used for experiment. The 650 nm laser diode (Model No.LD-780−5A) with 5 nm pulse width and optical output power ranging from 5 to 70 mW was used for the laser patterning.[33]

Fabrication of capacitor and Characterization. A Metal/GST/PVDF-TrFE/Al capacitors were made with a highly doped Si substrate as the bottom electrode and thermally evaporated Al top electrodes. Ferroelectric properties were obtained using a virtual ground circuit (Radiant Technologies Precision LC unit) at 100 Hz not elsewhere indicated.

Fabrication of FeFET and Characterization. Fabrication of a FeFET memory with single crystal TIPS-PEN active channel starts with the formation of a PVDF-TrFE gate dielectric (capacitance 14.6 nF cm^{-2}) on a heavily doped Si gate electrode. Single crystal Triisopropylsilylethynyl pentacene (TIPS-PEN) was then deposited on the PVDF-TrFE layer by solvent-exchange method described elsewhere.[9] A 70 nm thick and 200 μm square shape S/D Au electrodes were thermally evaporated through a shadow mask on the single crystal TIPS-PENs bridged between S/D electrodes. The electrical properties of the devices were recorded using semiconductor systems (E5270B, HP4284A, Agilent Technologies). All measurements were done in metallic shielded box at room temperature in air.

Microstructure Characterization. Scanning electron microscope (SEM) images were obtained with a JEOL JSM-600F. A 5 nm thick Pt layer was evaporated on a sample for contrast improvement. Optical microscope (OM) was used to visualize the patterned PVDF-TrFE thin film with Olympus BX 51M. 2-dimensional Grazing incident X-ray diffraction (GIXD) measurement was performed on the 4C2 beamline at the Pohang Accelerator Laboratory in Korea. The measurements were performed with monochromated X-rays (λ = 0.1381 nm) having grazing incidence angles ranging from 0.09 to 0.15 and the scattered intensity was recorded by SCX:4300−165/2 CCD detector (Princeton Instruments).

3. RESULTS AND DISCUSSION

Figure 1 shows a schematic of such a procedure of fabricating laser-induced PVDF-TrFE ferroelectric micropatterns. For the localized heat generation, we employed a 30 nm thick amorphous GST layer which has been widely used for optical information storage.[34−37] Heat is readily produced in the GST film upon exposure of 650 nm focused laser, followed by phase

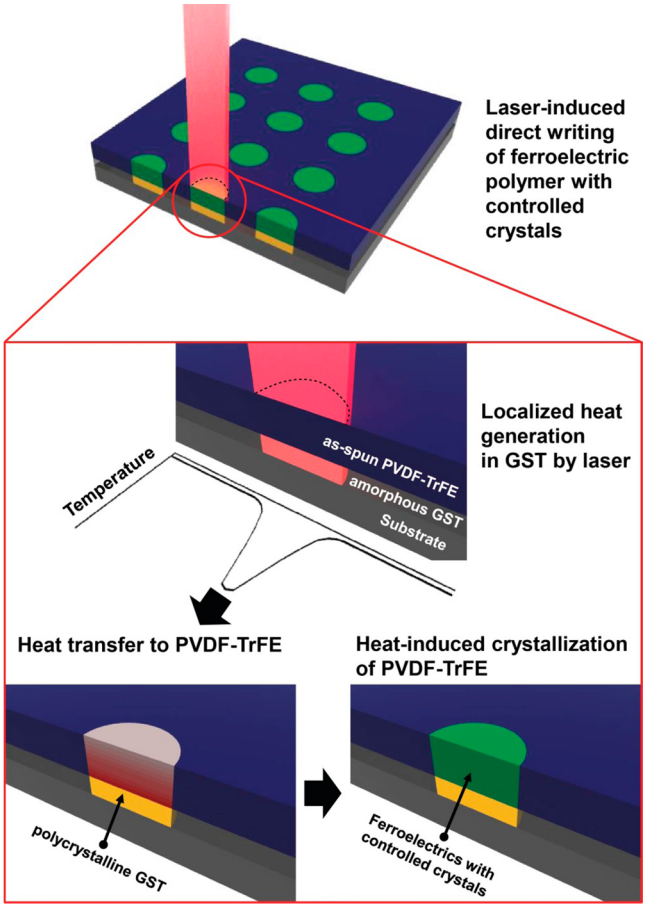

Figure 1. Schematic illustration of localized micropatterns of a PVDF-TrFE thin film using GST alloy layer with 650 nm focused laser. The sufficient heat is generated in GST layer upon laser exposure, giving rise to phase transformation of the GST layer from amorphous to polycrystalline state as shown in the red box. The heat subsequently transferred to PVDF-TrFE layer efficiently modifies the crystalline structure of PVDF-TrFE layer, leading to well-defined micropatterns of ferroelectric polymer with controlled crystals.

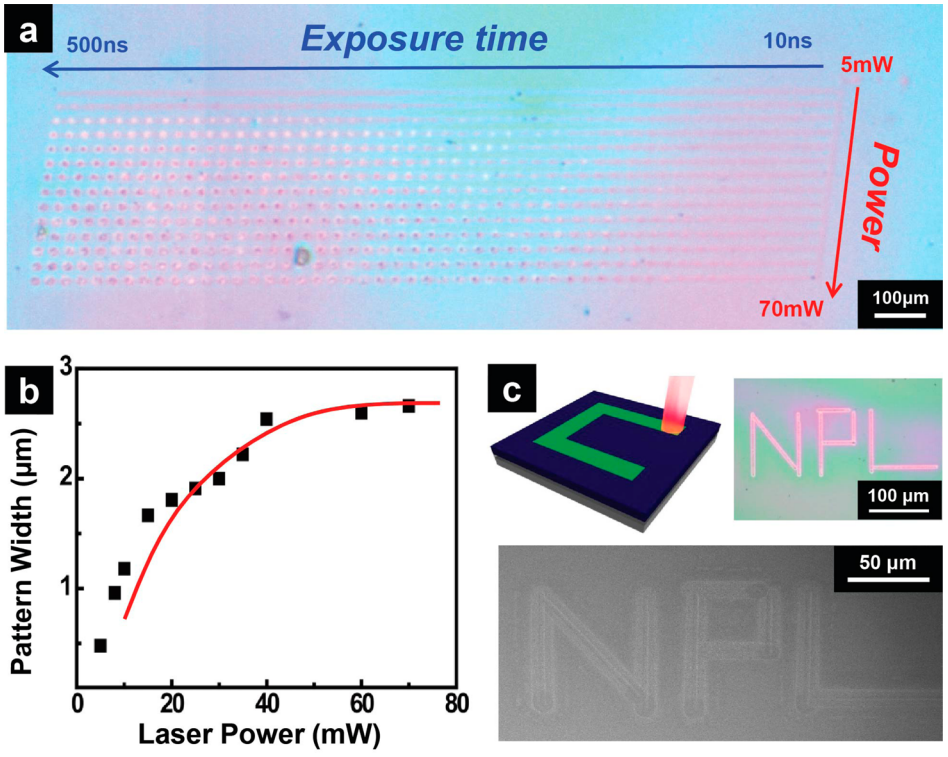

Figure 2. (a) The OM image of PVDF-TrFE thin film after irradiation of various laser conditions (exposure time and power). (b) Plot of pattern width (μm) vs laser power (mW) of PVDF-TrFE thin film. The exposed laser time is fixed for 500 ns. (c) Schematic, OM, and SEM images of charateristic patterns by using focused scanning laser.

transformation of the film from amorphous to crystalline state.[34−37] Different optical transmittance of the two phases allows one to read and write information. We employed the localized heat from GST to develop micropatterns of ferroelectric polymer. Fabrication of thin PVDF-TrFE micropatterns with GST can be made by the following three steps. First of all, localized heat with Gaussian distribution is generated in GST layer when it is irradiated by laser as shown in the scheme of Figure 1. Subsequently, the heat is sufficiently high over the glass transition temperature (T_g) of GST layer and thus can allow as-deposited amorphous state of GST layer to transform into crystalline state (the second step in the red box of Figure 1). The phase transformation of GST layer by focused laser was clearly observed even with 10 mW laser power (see the Supporting Information, Figure S1). The GST film underwent volume decrease of approximately 8% during phase transition from amorphous to polycrystalline phase.[38] The volume change of a 30 nm thick film in a confined region of a few micrometers gave rise to roughened surface topography as shown in the Supporting Information, S1. The RMS roughness of a film after laser exposure was approximately 5 nm. The heat in GST layer can be in turn transferred to thin PVDF-TrFE film as shown in the second step of the red box. As-spun PVDF-TrFE film without any prebaking steps can be thermally annealed in the local regions because of the focused heat and one can expect the improvement of degree of crystallization as well as crystal orientation of the film as shown in the third step of the red box of Figure 1.

Prior to the uptake experiment, we carried out a systematic study of PVDF-TrFE patterns developed on an approximately 450 nm thick polymer film by using direct writing with various exposing time from 10 to 500 ns and optical output power from 5 mW to 70 mW as shown in Figure 2a. In the OM image, the PVDF-TrFE pattern size monotonically increases from 500 nm to 2.5 μm with increasing applied laser power from 5 mW to 70 mW and expose time from 10 to 500 ns, respectively. The results of pattern size as a function of laser power are plotted as shown in Figure 2b. Apparently, there was no response of PVDF-TrFE film upon laser exposure when prepared on a bare Si wafer without GST as confirmed with UV−visible spectroscopy (see the Supporting Information, Figure S2). It is noted that the laser power below 30 mW for 500 ns expose time, the size of dot pattern is smaller than that of actual beam size of 2 μm. This indicates that the PVDF-TrFE has thermal response time after exposing the laser on GST substrate thus the sufficient power and time are prerequisite for developing precise size of ferroelectric patterns comparable with that of input laser beam. In contrast, with laser power greater than 30 mW, PVDF-TrFE pattern became 25% broader in size than 2 μm beam size mainly due to the Gaussian beam intensity profile of the highly intensified laser. We examined PVDF-TrFE films whose thickness ranged from 100 nm to 1 μm for laser-induced patterning. Below 100 nm in thickness, a film uniformly covered on a substrate was hardly obtained. Using this method, as proposed, we are able to create the micropattern of a thin PVDF-TrFE film with various shapes and width by scanning laser with controlled power and exposure time. For instance, alphabet letters of N, P, and L by our process can easily produce features on the micrometer-scale in Figure 2c.

The fabrication of PVDF-TrFE patterns as small as one can is of importance for ultrahigh density memory devices. By our patterning technique, we were able to reduce the pattern dimension to approximately 0.5 μm with 2 μm focused laser beam by carefully controlling both power and exposure time of the laser as shown in Figure 2a. We do believe that the pattern

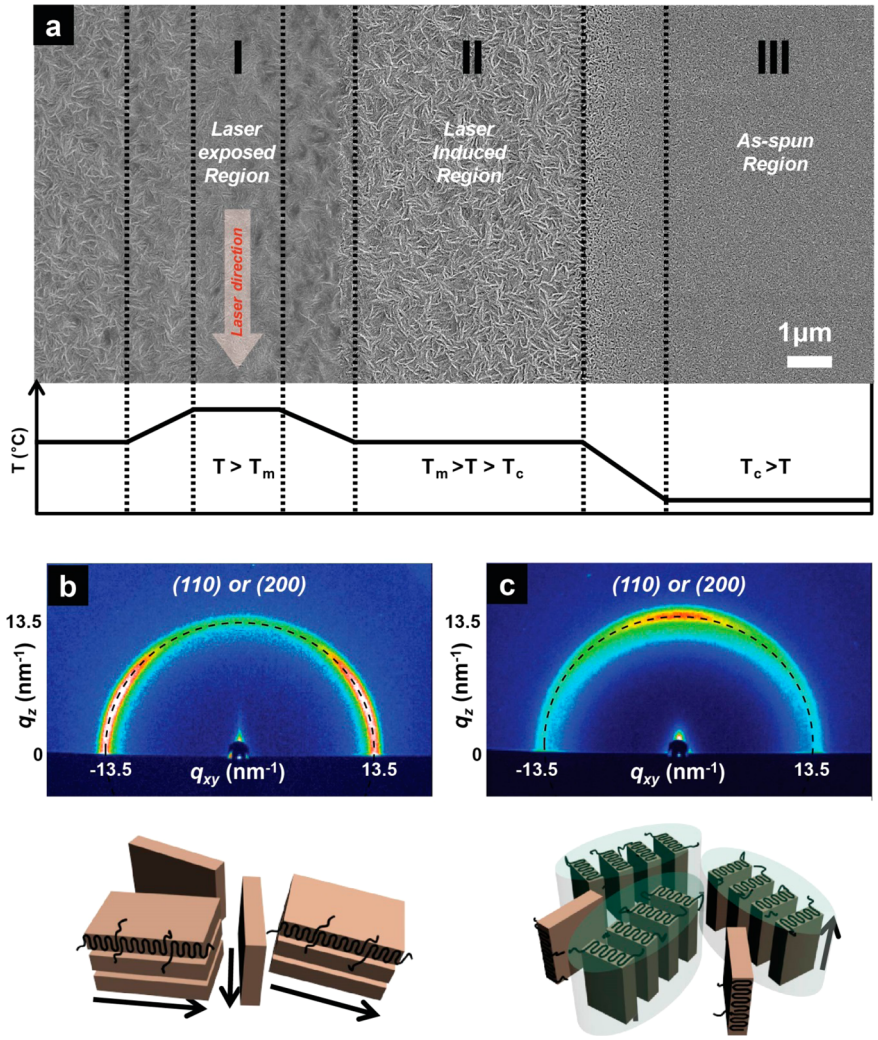

Figure 3. (a) SEM image of PVDF-TrFE thin film after exposure 50 mW power focused laser. In the below of SEM image shows the speculative temperature profile of each region. The GIXD images and proposed PVDF-TrFE crystal models corresponding to the images are shown in (b) region I and (c) region II. The dot circles in GIXD images added for clarity show the q value of (110) or (200) plane.

dimension can be further scaled down when a laser with the smaller beam size is used. In the literature, GST film can be readily patterned with its pattern size of approximately 50 nm with a focused laser in optical disk drives.[39] In addition, our patterning technique is still useful because nonvolatile polymer memory developed with the laser-induced patterned ferroelectric domains would compete with alternative memories based on printing technology suitable for flexible devices rather than conventional ultrahigh density ones on silicon patterning processes. Considering that most of printing technologies are limited to reduce pattern size below a few micron level, our technique is still beneficial.

To understand the effect of laser-induced heat on both molecular and microstructures of a PVDF-TrFE thin film, we performed SEM and 2D GIXD experiments as shown in Figure 3. For comparison, a spin-coated PVDF-TrFE thin film was thermally annealed at 135 °C for 2 h on hot plate (as shown in Figure S3 in the Supporting Information). The well-developed microdomains with closely packed, needle-like crystals are clearly observed in both SEM and GIXD, and the results are well-matched with other reports.[2,12] Figure 3a shows the characteristic microstructures of the PVDF-TrFE thin film on the GST layer after expose 50 mW power for 500 ns. As noted, there are three distinct morphology regions attributed to the localized heat generation from GST layer. The different morphology can be distinguished by temperature of substrate where the region I shows long and curly PVDF-TrFE crystal structure indicating that the actual temperature exerted on PVDF-TrFE is above its melting temperature (155 °C).[2,12] On the other hand, the common needle like crystal morphology is observed in region II which implies that the temperature of the ferroelectric film is between Curie and melting temperature of PVDF-TrFE. The morphology is also known as one favorable for ferroelectric polarization.[2,12] The characteristic needlelike morphology is fading from the center of laser beam and as-spun PVDF-TrFE film morphology is clearly visible as shown in region III. Considering the expose time of the laser, this method is extremely beneficial for reducing the conventional thermal annealing time. Ferroelectric crystals developed upon 7200 s thermal annealing in the reference sample were produced equivalently by our process with 0.5 μs laser exposure. The laser-induced patterning by GST was also suitable for various organic materials such as semiconducting small molecules, semiconducting polymer, amorphous and semicrystalline polymer (as shown in Figure S4 in the Supporting Information). It should be noted that the efficiency

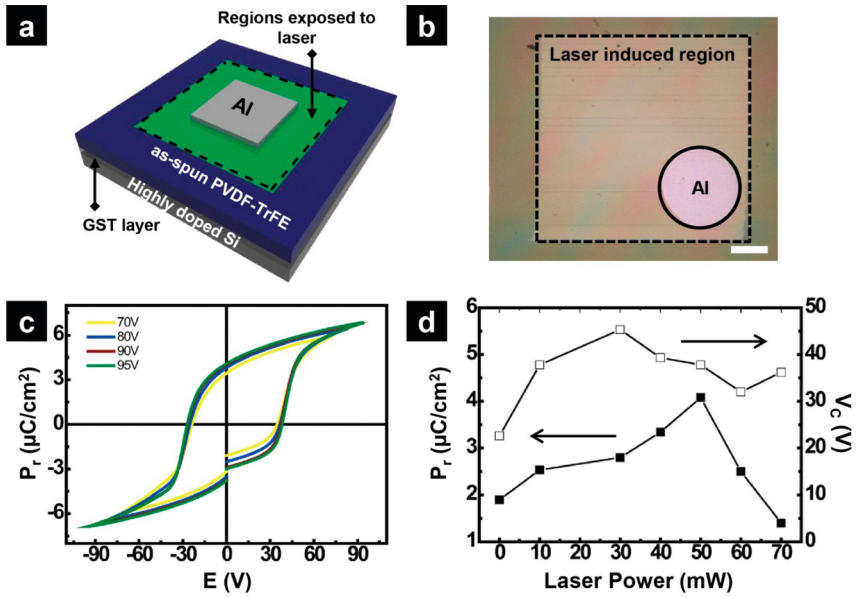

Figure 4. (a) Schematic illustration of the device architecture of a metal/GST/PVDF-TrFE/Al capacitor cell. (b) OM image of a capacitor device. The rectangular dots and black circle indicate the laser-induced region (50 mW power) and Al top electrode, respectively. The scale bar is 100 μm. (c) Polarization vs Voltage (P–V) curves of ferroelectric PVDF-TrFE thin film treated with focused laser. (d) Plots of P_r and V_c values of PVDF-TrFE capacitors as a function of laser irradiation power. The values were averaged over 10 cells.

of our process can be further justified when process time per patterned area is at the same time considered because temperature annealing is a massively parallel and extremely cheap. In this regard, our process can be still competitive when arrays of lasers are employed with much faster scanning rate. Rapid thermal laser annealing for polycrystalline Si can be an example in display industry.[40]

To furthor understand the crystal packing of PVDF-TrFE morphology from three different regions, cross-sectional planes of the film after laser exposure were investigated by GIXD measurement. Figure 3b shows the GIXD data from region I where the two strong reflection peaks are located at the equator which can be designated by (110) or (200) plane of the PVDF-TrFE crystals. The results show that the chain axis of PVDF-TrFE crystals, *c*-axis and ferroelectric polarization axis, *b*-axis are preferentially aligned, parallel, and perpendicular to the surface normal, respectively. This orientation was frequently observed in thin PVDF-TrFE films molten and recrystallized at room temperature.[2,12] We, therefore, hypothesize that after irradiating high power of 50 mW laser to GST, the temperature is steeply increased to above 150 °C. The microstructure of PVDF-TrFE film in the region I of Figure 3a is also consistent with that observed in a molten-recrystallized film. Due to thermal gradient from the center of the beam, the temperature in region II is believed to be lower than 150 °C, where PVDF-TrFE crystals favorable for ferroelectric polarization switching are evolved. As expected, the GIXD from region II shows that the (110) or (200) reflections are apparent in the meridian of the detector. The results exhibit that different from the crystalline structure of the region I, the chain axis of PVDF-TrFE crystals, *c*-axis and ferroelectric polarization axis, *b*-axis are preferentially aligned, perpendicular and parallel to the surface normal, respectively, indicating that the facile ferroelectric switching can occur with the PVDF-TrFE crystal orientation upon electric bias as shown next.

The laser-induced crystalline microstructures of PVDF-TrFE films were correlated with ferroelectric properties of the films. First of all, polarization applied voltage (P–E) hysteresis loop was measured by metal/GST/PVDF-TrFE/Al capacitors as shown in Figure 4. A PVDF-TrFE thin film were exposed by various laser power conditions from 10 mW to 70 mW for the area of 500 × 500 μm^2, followed by deposition of arrays of 200 μm diameter Al counter electrodes as representatively shown in Figure 4b. As expected by both SEM and GIXD measurement, the low remnant polarization (P_r) value of 1.89 μC/cm^2 was observed with as-spun PVDF-TrFE thin film. (as shown in Figure S5 in the Supporting Information). In contrast, laser treated PVDF-TrFE thin film with 50 mW power shows a remnant polarization of 4.08 μC/cm^2 and coercive voltage of 37 V with square-like count clockwise hysteresis loop as shown in Figure 4c. Further increase the laser power to 70 mW with which PVDF-TrFE film was molten and subsequently recrystallized gave rise to sudden drop of P_r due to the detrimental PVDF-TrFE chain orientation with respect to the electric bias direction as predicted in the GIXD results of Figure 3a (see the Supporting Information, Figure S5) Both coercive voltage and P_r values are plotted as a function of laser power in Figure 4d.

It is noteworthy that a capacitor with bilayered PVDF-TrFE/GST with the architecture of metal-ferroelectric-insulator–metal (MFIM) is treated as two independent and individual capacitors connected in series.[41] In this circumstance, the voltage applied should be shared with GST layer according to the series model, giving rise to the increase of the apparent coercive voltage as observed in our experiments. The effective coercive voltage applied only to the PVDF-TrFE film is, however, supposed to be same regardless of the interlayers. The coercive field of an approximately 450 nm thick PVDF-TrFE film used in the current work was approximately 53 MV/m which is in the range of most of coercive fields of PVDF-TrFE films reported. The coercive field was almost same regardless of film thickness in our sample when various MFM capacitors were investigated with different PVDF-TrFE film thickness as shown in the Supporting Information, Figure S6. It is also important to investigate the effect of GST layer on ferroelectric

switching of a PVDF-TrFE film, which can be characterized by frequency-dependent polarization switching of the film.[42,43] Frequency dependence of our ferroelectric PVDF-TrFE films on various surface conditions such as Al, highly doped Si, and GST are all similar in that the coercive field increases with frequency (see the Supporting Information, Figure S7). Although more detailed studies should be done over large range of frequency and temperature, the results we observed partly suggest that GST layer in contact with PVDF-TrFE rarely affects the intrinsic nucleation and growth of ferroelectric domains, considering that ferroelectric domain switching is dominantly initiated and propagated at both top and bottom surface of a thin ferroelectric film.

Although the results suggest that the 50 mW power intensity shows the highest remnant polarization with saturated hysteresis loop, the value is slightly lower than that of a capacitor with thermally annealed reference PVDF-TrFE film. (~5.4 μC/cm^2) A plausible explanation for this is that in spite of careful control of exposure time to minimize overheating of a PVDF-TrFE film above its melting temperature, the center of 50 mW focused laser generates the heat above melting temperature of PVDF-TrFE where the orientation is not favorable for chain rotation with respect to the electric bias.[2,12] Although the dominant contribution of the remnant polarization in the capacitor came from region II, the presence of region I in the 200 μm diameter Al top electrode may reduce the overall P_r in the cell. The different morphology of PVDF-TrFE crystalline observed with various laser irradiation power is also consistent with P-E results (see the Supporting Information, Figure S8).

Despite the relatively small remnant polarization, this laser-induced ferroelectric PVDF-TrFE crystals can be successfully used as an insulator in FeFET. To complete the FeFET devices, the ribbon-type single-crystalline TIPS-PEN organic semiconductor was used as shown schematically in Figure 5a. A TIPS-PEN single crystal was grown by solvent exchange method on the laser patterned PVDF-TrFE thin film and securely bridged between source and drain Au top-contact.[10] A well-saturated hysteresis of source−drain current (I_{DS}) was obtained as a function of gate bias voltage (V_G) because of the presence of ferroelectric PVDF-TrFE gate insulting layer as shown in Figure 5b. The accumulation of the excess holes in the p-type TIPS-PEN single crystal semiconductor in particular closed to the interface between TIPS-PEN and PVDF-TrFE layers raise the sharp increase of I_{SD} with negative gate voltage. After the removal of the negative gate voltage, the I_{SD} of approximately 1×10^{-7}. A still remains at the value saturated with the V_G of −60 V. The ON/OFF bistability of laser patterned FeFET device is approximately 1×10^5 at normal ambient conditions with a gate voltage sweep of ±60 V.

It should be noted that GST layer used as heat generator on top of gate electrode was also served as an additional insulator which significantly reduced gate leakage current between gate and drain electrode, leading to very low OFF state I_{DS} of approximately 1×10^{-12} A. It should be noted that upon exposure of a laser on a GST film, the electrical resistance of the film was significantly reduced from 1×10^8 Ohm to approximately 10^5 Ohm due to the nature of polycrystalline phase.[44] The polycrystalline film with the low resistance is not sufficiently conductive but still quite insulating, leading to the reduction of the OFF leakage current. The reliability of FeFET with laser patterned PVDF-TrFE was examined by data retention of both ON and OFF current state with time. We

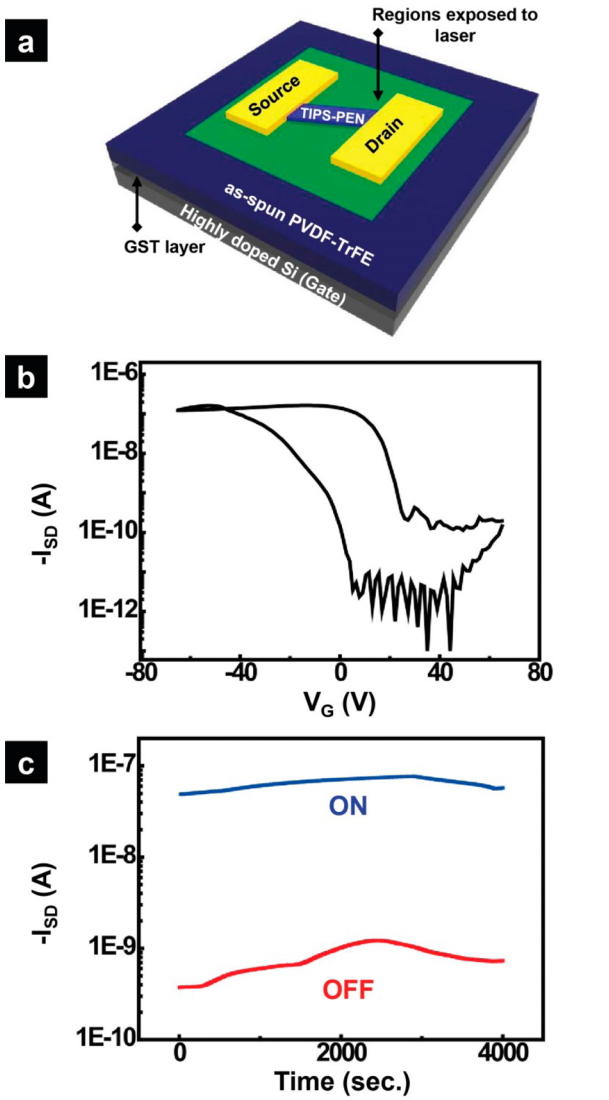

Figure 5. (a) Schematic illustration of the FeFET device architecture of a metal/GST/PVDF-TrFE/TIPS-Pentacene/Au cell. (b) Ferroelectric hysteresis loop of ferroelectric PVDF-TrFE with TIPS-PEN single crystal measured at V_D = −5 V. (c) Data retention of a FeFET memory with single crystal TIPS-PEN independently measured with the ON and OFF state drain current taken per second. The currents were detected at zero gate voltage with the continuous drain voltage of −5 V after single voltage pulse of −60 and +60 V for ON and OFF current, respectively.

independently measured nonvolatile I_{DS} values of ON and OFF states containing laser patterned PVDF-TrFE thin film under zero gate voltage with a constant source−drain voltage (V_{DS}) of −5 V. Both ON and OFF state currents were maintained longer than 4×10^3 seconds without any additional encapsulation as shown in Figure 5c.

It is of importance to properly separate adjacent ferroelectric memory cells with paraelectric insulator for practical application to avoid a possible cross-talk between the two cells.[45−47] It may be problematic because the regions between two micropatterns of a laser-exposed ferroelectric layer are still ferroelectric in spite of their low P_r of approximately 1.89 μC/cm^2. P_r value can be, however, significantly reduced in a FeFET architecture in which relatively low P_r is required to saturate in particular an organic semiconducting channel. In fact, the P_r values of a

MFIM capacitor containing unexposed PVDF-TrFE film were varied from 0 to approximately 0.4 $\mu C/cm^2$ when programmed from 0 to 60 V which corresponded to the voltage range for FeFET operation (see the Supporting Information, Figure S9). We assume that these levels of P_r can sufficiently suppress a possible cross talks between the cells. Furthermore, the realization of integrated ferroelectric memory cells without cross-talks requires not only properly patterned ferroelectric layer but also micropatterns of several other device components such as semiconductor and electrodes. In fact, our previous works are the parts of these efforts in which we have demonstrated new printing methods for fabricating micron-scale patterns of semiconducting channels.[48,49] With these techniques, we were able to develop arrays of FeFETs with patterned semiconductors with 4 in. wafer scale uniformity.[49] By putting together all the patterning techniques of both ferroelectric and semiconducting layers, we do believe that integrated memory cells can be realized near future.

4. CONCLUSIONS

In summary, we demonstrated an effective nondestructive way to develop micropatterns of thin ferroelectric PVDF-TrFE films with controlled crystals by using localized heat arising from GST alloy thin layer. The heat was triggered by 650 nm laser exposed on GST layer for hundreds of nanoseconds and subsequently transferred to PVDF-TrFE. Dependent upon temperature built in the films, ferroelectric polymer crystals were efficiently controlled in both degree of the crystallinity and the molecular orientations. By controlling exposure time and power of the scanned laser, we were able to create various ferroelectric micropatterns. Both memory diode and transistor cells with laser scanned ferroelectric polymer layers exhibited excellent nonvolatile memory performance, comparable with devices containing ferroelectric films thermally annealed at least for 2 h. Furthermore, our approach capable of generating heat in sub-microseconds can be readily combined with number of other functional organic materials to create the micropattern for the future electronic applications.

■ ASSOCIATED CONTENT

Supporting Information

UV−vis spectroscopy results, optical images, SEM images, GIXD data, and MFM results. This material is available free of charge via the Internet at http://pubs.acs.org/.

■ AUTHOR INFORMATION

Corresponding Authors

*E-mail cmpark@yonsei.ac.kr. Tel -82-2-2123-2833. Fax -82-2-312-5375.

*E-mail: seokjukang@gmail.com.

Notes

The authors declare no competing financial interest.

■ ACKNOWLEDGMENTS

The authors gratefully acknowledgment the financial support provided by the Agency for Defense Development under the contract UD110050GD. This research was also supported by the Second Stage of the Brain Korea 21 Project in 2006 and a Korea Science and Engineering Foundation (KOSEF) grant funded by the Ministry of Science and Technology (MEST), Republic of Korea (R11-2007-050-03001-0) and Seoul Science Fellowship. This work was supported by the National Research Foundation of Korea (NRF) grant funded by the Korea government (MEST) (2014R1A2A1A01005046).

■ REFERENCES

(1) Lovinger, A. J. Ferroelectric Polymers. *Science* **1983**, *220*, 1115−1121.

(2) Park, Y. J.; Bae, I.; Kang, S. J.; Chang, J.; Park, C. Control of Thin Ferroelectric Polymer Films for Non-Volatile Memory Applications. *IEEE Trans. Dielectr. Electr. Insul.* **2010**, *17*, 1135−1163.

(3) Yamauchi, N.; Kato, K.; Wada, T. Observation of Ferroelectricity in Very Thin Vinylidene Fluoride Trifluoroethylene Copolymer[P-(VDF-TrFE)] Films by High Frequency *C-V* Measurements of Al-SiO_2-P(VDF-TrFE)-SiO_2-Si Capacitors. *Jpn. J. Appl. Phys.* **1984**, *23*, L671−L673.

(4) Yamauchi, N. A Metal-Insulator-Semiconductor (MIS) Device Using a Ferroelectric Polymer Thin Film in the Gate Insulator. *Jpn. J. Appl. Phys.* **1986**, *25*, 590−594.

(5) Naber, R. C. G.; De Boer, B.; Blom, P. W. M.; De Leeuw, D. M. Low-Voltage Polymer Field-effect Transistors for Nonvolatile Memories. *Appl. Phys. Lett.* **2005**, *87*, 203509−1 − 203509−3.

(6) Kang, S. J.; Park, Y. J.; Bae, I.; Kim, K. J.; Kim, H.-C.; Bauer, S.; Thomas, E. L.; Park, C. Printable Ferroelectric PVDF/PMMA Blend Films with Ultralow Roughness for Low Voltage Non-Volatile Polymer Memory. *Adv. Funct. Mater.* **2009**, *19*, 2812−2818.

(7) Sekitani, T.; Zaitsu, K.; Noguchi, Y.; Ishibe, K.; Takamiya, M.; Sakurai, T.; Someya, T. Printed Nonvolatile Memory for a Sheet-Type Communication System *IEEE Trans. Electron Devices* **2009**, *56*, 1027−1035.

(8) Naber, R. C. G.; Tanase, C.; Blom, P. W. M.; Gelinck, G. H.; Marsman, A. W.; Touwslager, F. J.; Setayesh, S.; De Leeuw, D. M. High-Performance Solution-processed Polymer Ferroelectric Field-Effect Transistors. *Nat. Mater.* **2005**, *4*, 243−248.

(9) Kang, S. J.; Bae, I.; Park, Y. J.; Park, T. H.; Sung, J.; Yoon, S. C.; Kim, K. H.; Choi, D. H.; Park, C. Non-volatile Ferroelectric Poly(vinylidene fluoride-*co*-trifluoroethylene) Memory Based on a Single-Crystalline Tri-isopropylsilylethynyl Pentacene Field-Effect Transistor. *Adv. Funct. Mater.* **2009**, *19*, 1609−1616.

(10) Kang, S. J.; Bae, I.; Shin, Y. J.; Park, Y. J.; Huh, J.; Park, S.-M.; Kim, H.-C.; Park, C. Nonvolatile Polymer Memory with Nanoconfinement of Ferroelectric Crystals. *Nano Lett.* **2011**, *11*, 138−144.

(11) Baeg, K.-J.; Khim, D.; Kim, J.; Yang, B.-D.; Kang, M.; Jung, S.-W.; You, I.-K.; Kim, D.-Y.; Noh, Y.-Y. High-Performance Top-Gated Organic Field-Effect Transistor Memory using Electrets for Monolithic Printed Flexible NAND Flash Memory. *Adv. Funct. Mater.* **2012**, *22*, 2915−2926.

(12) Park, Y. J.; Kang, S. J.; Park, C.; Kim, K. J.; Lee, H. S.; Lee, M. S.; Chung, U.; Park, I. J. Irreversible Extinction of Ferroelectric Polarization in P(VDF-TrFE) Thin Films upon Melting and Recrystallization. *Appl. Phys. Lett.* **2006**, *88*, 242908−1−242908−3.

(13) Tsutsumi, N.; Yoda, S.; Sakai, W. Infrared Spectra and Ferro-Electricity of Ultra-Thin Films of Vinylidene Fluoride and Trifluoro-ethylene Copolymer. *Polym. Int.* **2007**, *56*, 1254−1260.

(14) Kang, S. J.; Park, Y. J.; Sung, J.; Jo, P. S.; Park, C.; Kim, K. J.; Cho, B. O. Spin Cast Ferroelectric Beta Poly(vinylidene fluoride) Thin Films via Rapid Thermal Annealing. *Appl. Phys. Lett.* **2008**, *92*, 012921−1−012921−3.

(15) Kang, S. J.; Park, Y. J.; Hwang, J.; Jeong, H. J.; Lee, J. S.; Kim, K. J.; Kim, H.; Huh, J.; Park, C. Localized Pressure-Induced Ferroelectric Pattern Arrays of Semicrystalline Poly(vinylidene fluoride) by Microimprinting. *Adv. Mater.* **2007**, *19*, 581−586.

(16) Hu, Z.; Baralia, G.; Bayot, V.; Gohy, J.-F.; Jonas, A. M. Nanoscale Control of Polymer Crystallization by Nanoimprint Lithography. *Nano Lett.* **2005**, *5*, 1738−1743.

(17) Steinhart, S.; Senz, S.; Wehrspohn, R. B.; Gösele, U.; Wendorff, J. H. Curvature-Directed Crystallization of Poly(vinylidene difluoride) in Nanotube Walls. *Macromolecules* **2003**, *36*, 3646−3651.

(18) Steinhart, M.; Göring, P.; Dernaika, H.; Prabhukaran, M.; Gösele, U.; Hempel, E.; Thurn-Albrecht, T. Coherent Kinetic Control over Crystal Orientation in Macroscopic Ensembles of POLYMER

Nanorods and Nanotubes. *Phys. Rev. Lett.* **2006**, *97*, 027801−1−027801−4.
(19) Zhang, L.; Ducharme, S.; Li, J. Microimprinting and Ferroelectric Properties of Poly(vinylidene fluoride-trifluoroethylene) Copolymer Films. *Appl. Phys. Lett.* **2007**, *91*, 172906−1 − 172906−3.
(20) Bai, M.; Ducharme, S. Ferroelectric Nanomesa Formation from Polymer Langmuir-Blodgett Films. *Appl. Phys. Lett.* **2004**, *85*, 3528−1−3528−3.
(21) Hu, Z.; Tian, M.; Nysten, B.; Jonas, A. M. Regular Arrays of Highly Ordered Ferroelectric Polymer Nanostructures for Non-Volatile Low-Voltage Memories. *Nat. Mater.* **2008**, *8*, 62−67.
(22) Nougaret, L.; Kassa, H. G.; Cai, R.; Patois, T.; Nysten, B.; van Breeman, A. J. J. M.; Gelinck, G. H.; de Leeuw, D. M.; Marrani, A.; Hu, Z.; Jonas, A. M. Nanoscale Design of Multifunctional Organic Layers for Low-Power High-Density Memory Devices. *ACS Nano* **2014**, *8*, 3498−3505.
(23) Park, Y. J.; Kang, Y. S.; Park, C. Micropatterning of Semicrystalline Poly(vinylidene Fluoride) (PVDF) Solutions. *Eur. Polym. J.* **2005**, *41*, 1002−1012.
(24) Asadi, K.; de Leeuw, D. M.; Boer, B. D.; Blom, P. W. M. Organic Non-volatile Memories from Ferroelectric Phase-separated Blends. *Nat. Mater.* **2008**, *7*, 547−550.
(25) Cauda, V.; Torre, B.; Falqui, A.; Canavese, G.; Stassi, S.; Bein, T.; Pizzi, M. Confinement in Oriented Mesopores Induces Piezoelectric Behavior of Polymeric Nanowires. *Chem. Mater.* **2012**, *24*, 4215−4221.
(26) Cauda, V.; Stassi, S.; Bejtka, K.; Canavese, G. Nanoconfinement: an Effective Way to Enhance PVDF Piezoelectric Properties. *ACS Appl. Mater. Interfaces* **2013**, *5*, 6430−6437.
(27) Wu, Y.; Gu, Q.; Ding, G.; Tong, F.; Hu, Z.; Jonas, A. M. Confinement Induced Preferential Orientation of Crystals and Enhancement of Properties in Ferroelectric Polymer Nanowires. *ACS Macro Lett.* **2013**, *2*, 535−538.
(28) Morikawa, E.; Choi, J.; Manohara, H. M.; Ishii, H.; Seki, K.; Okudaira, K. K.; Ueno, N. Photoemission Study of Direct Photomicromachining in Poly(vinylidene fluoride). *J. Appl. Phys.* **2000**, *87*, 4010−1 − 4010−7.
(29) Choi, J.; Manohara, H. M.; Morikawa, E.; Sprunger, P. T.; Dowben, P. A.; Palto, S. P. Thin Crystalline Functional Group Copolymer Poly(vinylidene fluoride-trifluoroethylene) Film Patterning Using Synchrotron Radiation. *Appl. Phys. Lett.* **2000**, *76*, 381−1 − 381−3.
(30) Bystrov, V. S.; Bdikin, I. K.; Kiselev, D. A.; Yudin, S.; Fridkin, V. M.; Kholkin, A. L. Nanoscale Polarization Patterning of Ferroelectric Langmuir-Blodgett P(VDF-TrFE) Films. *J. Phys. D: Appl. Phys.* **2007**, *40*, 4571−4577.
(31) Rodriguez, B. J.; Jesse, S.; Kalinin, S. V.; Kim, J.; Ducharme, S.; Fridkin, V. M. Nanoscale Polarization Manipulation and Imaging of Ferroelectric Langmuir-Blodgett Polymer Films. *Appl. Phys. Lett.* **2007**, *90*, 122904−1 − 122904−3.
(32) Rankin, C.; Chou, C.; Conklin, D.; Bonnell, D. A. Polarization and Local Reactivity on Organic Ferroelectric Surfaces: Ferroelectric Nanolithography Using Poly(vinylidene fluoride). *ACS Nano* **2007**, *1*, 234−238.
(33) Acharya, H.; Yoon, B.; Park, Y. J.; Bae, I.; Park, C. Block Copolymer Micelles with Near Infrared Metal Phthalocyanine Dyes for Laser Induced Writing. *Macromol. Rapid Commun.* **2010**, *31*, 1071−1077.
(34) Wuttig, M.; Yamada, N. Phase-Change Materials for Rewriteable Data Storage. *Nat. Mater.* **2007**, *6*, 824−832.
(35) Chu, C. H.; Shiue, C. D.; Cheng, H. W.; Tseng, M. L.; Chiang, H.-P.; Mansuripur, M.; Tsai, D. P. Laser-Induced Phase Transitions of $Ge_2Sb_2Te_5$ Thin Films Used in Optical and Electronic Data Storage and in Thermal Lithography. *Opt. Exp.* **2010**, *18*, 18383−18393.
(36) Deng, C.; Geng, Y.; Wu, Y.; Wang, Y.; Wei, J. Adhesion Effect of Interface Layers on Pattern Fabrication with GeSbTe as Laser Thermal Lithography Film. *Microelectron. Eng.* **2013**, *103*, 7−11.
(37) Kumar, S.; Singh, D.; Thangaraj, R. Structural, Electrical and Optical Study of Thermally Evaporated $Ge_8Sb_2Te_{11}$ Thin Films. *Thin Solid Films* **2013**, *531*, 577−582.
(38) Lyeo, H.-K.; Cahill, D. G.; Lee, B.-S.; Abelson, J. R.; Kwon, M.-H.; Kim, K.-B.; Bishop, S. G.; Cheong, B. Thermal Conductivity of Phase-change material $Ge_2Sb_2Te_5$. *Appl. Phys. Lett.* **2006**, *89*, 151904−1 − 151904−3.
(39) Lin, Y.; Hong, M. H.; Chong, T. C.; Lim, C. S.; Chen, G. X.; Tan, L. S.; Wang, Z. B.; Shi, L. P. Ultrafast-laser-induced Parallel Phase-change Nanolithography. *Appl. Phys. Lett.* **2006**, *89*, 041108−1 − 041108−3.
(40) Fiebig, M.; Osmanov, R.; Stamm, U.; Frank, V.; Oesterlin, P.; Kobayashi, N.; Fechner, B.; Uzuka, L. High-power Excimer Lasers for High-throghput Poly-Si Annealing. *Int. Soc. Opt. Photonics* **2000**, *3888*, 464−469.
(41) Chang, J.; Shin, C. H.; Park, Y. J.; Kang, S. J.; Jeong, H. J.; Kim, K. J.; Hawker, C. J.; Russell, T. P.; Ryu, D. Y.; Park, C. Polymeric Gate Dielectric Interlayer of Cross-linkable Poly(styrene-r-methylmethacrylate) Copolymer for Ferroelectric PVDF-TrFE Field Effect Transistor Memory. *Org. Electron.* **2009**, *10*, 849−856.
(42) Horiuchi, S.; Tokunaga, Y.; Giovannetti, G.; Picozzi, S.; Itoh, H.; Shimano, R.; Kumai, R.; Tokura, Y. Above-room-temperature Ferroelectricity in a Single-component Molecualr Crystal. *Nature* **2010**, *463*, 789−792.
(43) Hu, W. J.; Juo, D.-M.; You, L.; Wang, J.; Chen, Y.-C.; Chu, Y.-H.; Wu, T. Universal Ferroelectric Switching Dynamics of Vinylidene Fluoride-trifluoroethyene Copolymer Films. *Sci. Rep.* **2014**, *4*, 1−8.
(44) Li, X. Z.; Yoon, J.; Lee, D.; Kim, S.; Kim, K.-B.; Park, Y. J. Developing the Electrode Board for Bio Phase Change Template. *Korean Chem. Eng. Res.* **2009**, *47*, 715−719.
(45) Kim, B. H.; Byun, C. W.; Yoon, S.-M.; Yang, S. H.; Jung, S. H.; Jung, S.-W.; Ryu, M. K.; Park, S.-H. K.; Hwang, C.-S.; Cho, K.-I.; Kwon, O.-S.; Park, E.-S.; Oh, H. C.; Kim, K.-H.; Park, K. C. Oxide-Thin-Film-Transistor-Based Ferroelectric Memory Array. *IEEE Electron Device Lett.* **2011**, *32*, 324−326.
(46) Ng, T. N.; Russo, B.; Krusor, B.; Kist, R.; Arias, A. C. Organic Inkjet-patterned Memory Array Based on Ferroelectric Field-effect Transistors. *Org. Elec.* **2011**, *12*, 2012−2018.
(47) Kim, M.-H.; Lee, G. J.; Keum, C.-M.; Lee, S.-D. Concept of Rewritable Organic Ferroelectric Random Access Memory in Two Lateral Transistors-in-one Cell Architecture. *Semicond. Sci. Technol.* **2014**, *29*, 025004−1 − 025004−6.
(48) Bae, I.; Kang, S. J.; Shin, Y. J.; Park, Y. J.; Kim, R. H.; Mathevet, F.; Park, C. Tailored Single Crystals of Triisopropylsiylethynyl Pentacene by Selective Contact Evaportaion Printing. *Adv. Mater.* **2011**, *23*, 3398−3402.
(49) Bae, I.; Hwang, S. K.; Kim, R. H.; Kang, S. J.; Park, C. Wafer-Scale Arrays of Nonvolatile Polymer Memories with Microprinted Semiconducting Small Molecule/Polymer Blends. *ACS Appl. Mater. Interfaces* **2013**, *5*, 10696−10704.